Evolutionary rescue over a fitness landscape

Yoann Anciaux[1], Luis-Miguel Chevin[2], Ophélie Ronce[1], and Guillaume Martin[1]

[1] Institut des Sciences de l'Evolution de Montpellier (UMR 5554 ISE-M), CNRS – Université Montpellier 2, Place Eugène Bataillon, 34095 Montpellier Cedex 05, France

[2] Centre d'Ecologie Fonctionnelle et Evolutive (UMR 5175), 1919 route de Mende, 34293 Montpellier Cedex 5, France

Contact : yoann.anciaux@umontpellier.fr

Keywords : Antibiotic resistance; Evolutionary rescue; Fisher's Geometric Model; Fitness landscape; Mutation

Abstract

Evolutionary rescue describes a situation where adaptive evolution prevents the extinction of a population facing a stressing environment. Models of evolutionary rescue could in principle be used to predict the treatment levels most likely to limit the emergence of resistance in pests or pathogens. Stress levels are known to affect both the rate of decline of the population (demographic effect) and the speed of adaptation to the stressing environment (evolutionary effect), but the latter aspect has received less attention. Here, we derive a model of evolutionary rescue that includes both effects, using Fisher's Geometric Model of adaptation. In this model, the fitness effects of mutations depend both on the genotype and environment in which they arise. In particular, the model introduces a dependence between the proportion of rescue mutants, or their cost, and the level of stress. Analytic results were obtained under a strong selection weak mutation regime, and their accuracy was tested by simulations. Stress can affect different parameters of the fitness landscape in our model, which are amenable to empirical measurements. These effects can be summarized into a single composite parameter, measuring stress intensity. Using this composite parameter, we describe a narrow 'characteristic stress window' of stress levels, over which the rescue probability drops from very likely to very unlikely. The rescue probability drops more sharply with increasing stress than in previous models without context-dependent mutation. We discuss how to test these predictions with rescue experiments across gradients of stress.

Introduction

Understanding the persistence or decline to extinction of populations is a crucial challenge both for the conservation of biodiversity and the eradication of pests or pathogens (Gonzalez *et al.* 2013; Carlson *et al.* 2014; Alexander *et al.* 2014). In evolutionary biology, 'environmental stress' broadly characterizes an environment that induces a reduction in fitness

for organisms (Koehn and Bayne 1989; Bijlsma and Loeschcke 2005). Here, we will focus on the case where environmental stress causes a reduction of population mean fitness that is harsh enough to trigger a decline in abundance (Hoffmann and Parsons 1997). In such a stressful environment, if heritable variation in fitness is available or arises by mutation, then adaptive evolution may allow the population to escape extinction. This phenomenon has been called 'evolutionary rescue' (ER) (Gomulkiewicz and Holt 1995). Evolutionary rescue is of particular importance to understand the emergence of genetic resistance to drugs or treatments in medicine and agronomy (Davies and Davies 2010).

Empirical evidence supports the idea that stress levels critically determine ER probabilities (Samani and Bell 2010; Moser and Bell 2011; Lindsey *et al.* 2013). For example, the probability of antibiotic resistance emergence in bacteria (that is, the probability to avoid antibiotic-induced extinction through ER) typically declines sharply, in a strongly non-linear way, with increasing drug concentration (Drlica 2003). Evolutionary rescue thus shifts from being highly likely to highly unlikely over a narrow window of stress level. This critical range of stress depends on the strain, especially on its evolutionary history with respect to exposure to the stress (Gonzalez and Bell 2013). Stress level, as controlled by the drug concentration, was also shown to affect the genetic basis of resistance (e.g. in Harmand *et al.* 2016), with a wider diversity of genes and alleles conferring resistance at low dose than at high doses. However, the underlying causes for this relationship between stress level and the probability/genetic basis of ER is still poorly understood, challenging our ability to predict these eco-evolutionary dynamics. Our aim here is to derive new analytical predictions for the relationship between ER and stress level, predicting in particular the critical window of stress levels above which ER is very unlikely, and allowing direct comparison with experimental data.

In the theoretical literature (reviewed in Alexander *et al.* 2014), most ER models indeed predict a dependence of ER probability on stress levels, as measured by the decay rate of the stressed population. Indeed, higher stress levels directly impose a faster decay to extinction. This leaves less time for the population to adapt before extinction, be it by rare *de novo* mutations (e.g. Orr and Unckless 2008) or through standing genetic variance (e.g. Gomulkiewicz and Holt 1995). Some model however predict that, when adaptation stems from rare pre-existing mutants (e.g. standing variance model in Orr and Unckless 2008, 2014), the initial decay rate of the population does not impact rescue probabilities.

Stress level may also have indirect effects on ER. Indeed, a stressful environment may not only affect the demographic properties of the population, but also its rate of adaptation

(Hoffmann and Parsons 1997; De Visser and Rozen 2005; Agrawal and Whitlock 2010). The rate of mutations and the distribution of their effects on fitness change across environments (Martin and Lenormand 2006b; Wang *et al.* 2009; Agrawal and Whitlock 2010; Wang *et al.* 2014). In particular, the fraction of beneficial mutations was found to increase in stressful environments (Remold and Lenski 2001, 2004). Standing variation for quantitative traits, and in particular fitness components, also frequently depends on the environment where it is measured (Hoffmann and Merilä 1999; Sgrò and Hoffmann 2004; Charmantier and Garant 2005). Finally, the initial frequency of preexisting variants able to rescue the population from extinction in a stressful environment depends on their selective cost in the past environment. Variations in this cost across stress levels (i.e. between mutations conferring resistance to different levels), could induce corresponding variations in ER probability. In light of this empirical evidence, it seems clear that progress towards understanding and predicting ER across stress levels requires addressing, in a quantitative way, the joint effect of stress on the demography and genetic variation of population exposed to stressful conditions. This is our goal in the present article.

To do so, we develop a model that is hybrid between two modeling traditions in ER theory, summarized by Alexander et al. (2014): discrete genetic models, and quantitative genetics models. Discrete genetic models assume a narrow genetic basis for adaptation (and ER), whereby a single beneficial mutation can rescue an otherwise monomorphic population (Orr and Unckless 2008; Martin *et al.* 2013; Uecker *et al.* 2014; Orr and Unckless 2014; Uecker and Hermisson 2016). This approach was initially proposed for ER by Gomulkiewicz and Holt (1995), and later extended to account for (i) evolutionary and demographic stochasticity (e.g. Orr and Unckless 2008), and (ii) variation in the selection coefficients of mutations that may cause a rescue, with an arbitrary distribution of fitness effects (Martin *et al.* 2013). However, such models do not predict how the fitness effects of mutations vary with stress level, i.e. how the genetic and/or environmental context determine these effects. For this reason, they make it difficult to jointly address the two fundamental components of stress mentioned above. On the contrary, quantitative genetics models inherently address the influence of stress on the rate of adaptation by assuming that adaptation (and ER) is caused by evolution of a quantitative trait whose optimum changes with the environment (Lynch *et al.* 1991; Burger and Lynch 1995; Gomulkiewicz and Holt 1995). In these models, both the rate of decline and the rate of adaptation in the stressful environment depend on the distance between the phenotypic optima in the past and present environments. However, analytical predictions were derived assuming a broad, polygenic basis for adaptation with a stable genetic variance of the quantitative trait. The

population genetic processes underlying adaptation were not explicitly modelled, and the stochasticity involved in fixation and establishment neglected. These complications were only explored by simulations (e.g. Gomulkiewicz *et al.* 2010).

In order to take the best of both approaches, we rely on Fisher's (1930) Geometrical Model (hereafter "FGM"), which predicts how the selective coefficients of mutations change across environments (and stress levels). Variation in fitness in the FGM is assumed to emerge from variation on multiple putative traits, undergoing stabilizing selection that depends on the environment. This model allows analytical tractability, while retaining various aspects of realism (reviewed in Tenaillon 2014). In particular, it predicts accurately how fitness effects of mutations change across environments (Martin and Lenormand 2006b; Hietpas *et al.* 2013; Harmand *et al.* 2016), or genetic backgrounds (Martin *et al.* 2007; MacLean *et al.* 2010; Trindade *et al.* 2012). Here, we combine this FGM with population genetic approaches that account for demographic and evolutionary stochasticity (Martin *et al.* 2013). The distribution of the demographic parameters of mutant genotypes then depends on both the genotype in which they arise, and on the environment in which they are expressed. Importantly, the FGM also predicts the covariation of selection coefficients across environments (Martin and Lenormand 2015). This creates a tractable connection, across stress levels, between (i) the decay rate, (ii) the rate and effect of rescue mutants, and (iii) their potential costs in the original environment, before the onset of stress.

We here use the FGM to analyze how the demographic and evolutionary effects of stress level affect evolutionary rescue caused by individual mutations. We consider either rescue from de novo mutations, or from standing variance at mutation-selection balance. We model evolutionary rescue in large asexual populations, similar to bacterial populations exposed to antibiotics, or populations of cancerous cells exposed to chemotherapy. Following (Martin *et al.* 2013), we use diffusion approximations, which can accommodate various demographic models. Explicit analytical approximations are obtained for an initially large asexual population undergoing relatively harsh stress, and checked against stochastic simulations. Our approximations assume that selection is strong and mutations rare (Gillespie 1983). In all cases, we predict a narrow window of stress levels over which evolutionary rescue shifts from being highly likely to highly unlikely. This window can be computed from experimentally measurable quantities. Our model integrates the different effects of stress on the demography and genetic variation for fitness and interestingly shows that these effects can be approximately summarized into a single composite measure that captures the 'effective stress level'. When measured on

this scale, the critical stress window depends only on the initial population size and the mutation rate.

Methods

In this section, we detail the assumptions of the model and the approximations used for its mathematical analysis, in terms of environmental change, eco-evolutionary dynamics and mutational model.

Abrupt environmental shift: We define two environments: (1) a non-stressful one, denoted as "previous environment", in which the population has a positive mean growth rate, and a large enough population size that demographic stochasticity can be ignored; and (2) a stressful one, denoted "new environment", in which the population initially has a negative mean growth rate, and the population size is subject to demographic stochasticity. Conditions shift abruptly from the previous to the new environment at $t = 0$, at which time the population size is N_0.

Eco-evolutionary dynamics: Extinction or rescue ultimately depends on details of the stochastic population dynamics of each genotype, which are here assumed to be mutually independent (no density or frequency – dependence see Chevin (2011)). As in Martin *et al.* (2013), we approximate these dynamics by a Feller diffusion (Feller 1951). This approximation reduces all the complexity of the life cycle into two key parameters for each genotype i: the expected growth rate r_i (our 'fitness' here), and the variance in reproductive output σ_i. As an illustration, our simulations below assume discrete generations and Poisson offspring distributions, wherein $\sigma_i = 1 + r_i \approx 1$ for any genotype, as long as their growth rates is not too large ($r_i \ll 1$, in per-generation time units, see **Appendix 1** and Martin *et al.* (2013)). As detailed in Martin *et al.* (2013), this diffusion approximation requires density-independent and 'smooth' demographic processes (moderate growth or decay).

To cause a rescue, a resistant mutant ($r_i > 0$) must 'establish', by avoiding extinction when rare. The probability that this happens, for a lineage with growth rate $r_i > 0$, starting in single copy (i.e., ignoring later mutations) is $\pi_F(r_i) = 1 - e^{-2\,r_i} \approx 2\,r_i$ (still assuming $r_i \ll \sigma_i$, with $\sigma_i \approx 1$ in the example used in simulations). We ignore stochasticity in the decay dynamics of the subpopulation of all non-resistant genotypes ($r_i < 0$). This is accurate as long as this subpopulation has large initial size, of order $N_0 \gg 1$ (Martin *et al.* 2013).

Finally, we assume that mutation rates per capita per unit time are constant over time. This is exact in models with discrete generations, but is only approximate in continuous-time models, where mutations occur during birth events, leading to higher mutation rates per unit time for genotypes with larger birth rates. The approximation then applies if birth and death rates are large relative to growth rates (birth minus death), which is also required to approximate birth death processes by a Feller diffusion (discussed Martin *et al.* 2013).

ER from standing variance vs. *de novo* mutation: At the onset of stress ($t = 0$), the population either consists of a single 'ancestral' clone, or is polymorphic at mutation-selection equilibrium in the previous environment. In the first case, we must derive the distribution of fitness effects, in the new environment, of mutants arising in the ancestral clone. In the second case, we must describe the potential rescue variants already present in the previous environment, plus the range of mutants that they may generate *de novo* after the onset of stress.

House-of-Cards approximation: We are interested in modeling the context-dependence of mutation fitness effects, in order to capture the different effects of stress described above. However, this context dependence implies epistasis, which makes the problem highly intractable in general. To make analytical progress, we assume a regime of strong selection and weak mutation rate (SSWM, Gillespie 1983), which allows substantial simplification. This regime arises when mutation rates are small relative to their typical effect (as detailed below). In our context, this assumption implies that most rescue variants are only one mutational step away from the (non-rescue) background in which they arise, such that we can ignore the accumulation of multiple mutations causing ER.

When considering a population initially at mutation-selection balance, the SSWM regime allows for further key simplifications. At mutation-selection balance, the equilibrium phenotype and fitness distributions both depend on a complex interplay between deleterious and compensatory mutations. However, in the SSWM regime, most segregating phenotypes remain within a narrow neighborhood of the phenotype that is optimal in the previous environment (the fittest genotype). We can thus derive the mutation-selection balance distribution of phenotypes and fitness by assuming that all mutations in each generation originate from the optimum phenotype in the previous environment. This is essentially the House-of-Cards approximation (Turelli 1984; Martin and Roques 2016) extended to the FGM in arbitrarily many dimensions (Martin and Roques 2016).

Under this assumption, ER from standing variance depends on the fitness distribution of variants, at mutation-selection balance in the previous environment. ER from *de novo* mutations depends on the distribution of fitness effects among mutants arising from the previous optimum phenotype as the only wild-type. We can thus directly borrow the results from Martin et al. (Martin *et al.* 2013), which are based on an arbitrary joint distribution of fitness effects in the new and the previous environment. The problem thus reduces to computing this joint distribution of fitness effects in the FGM, for random mutations arising in a single 'ancestral clone' that is optimal in the previous environment.

Context dependent mutations under Fisher's geometrical model (FGM): In any environment, growth rate (Malthusian fitness, or log fitness in discrete-time models) is assumed to be a quadratic function of n quantitative (continuous) phenotypic traits. The breeding values (heritable components) for these traits are concatenated in a vector $\mathbf{z} \in \mathbb{R}^n$, with optimum multivariate phenotype $\mathbf{z}_*$, at which the maximal growth rate is r_{max}. All genotypes are assumed to have the same stochastic variance in reproductive success (see above), leading to

$$\begin{array}{c} r(\boldsymbol{z}) = r_{max} - \|\boldsymbol{z} - \boldsymbol{z}_*\|^2/2 \\ \sigma(\mathbf{z}) \approx \sigma \gg r(\mathbf{z}), \text{for all } \mathbf{z} \end{array} . \qquad [1]$$

Assuming single peak in the phenotype-fitness landscape in each environment, the optimum in the new environment is set at $\mathbf{z}_* = \mathbf{0}$ without loss of generality. The optimum in the previous environment is set equal to the phenotype of the ancestral ('A') mean phenotype $\mathbf{z}_* = \mathbf{z}_A$. When starting from a clone, the previous environment is irrelevant, only the maladaptation of this clone counts. When starting from a population initially at mutation-selection balance, following the House-of-Cards approximation above, we also consider that all mutations emerge from the optimal phenotype in the previous environment, $\mathbf{z}_* = \mathbf{z}_{\boldsymbol{A}}$. The fitness of the ancestral clone in the new environment is $r(\mathbf{z}_A) = r_{max} - \|\boldsymbol{z}_{\boldsymbol{A}}\|^2/2 = -r_D$, where r_D is its rate of decay. This means that stress involves a shift of the optimum (from $\mathbf{z}_* = \mathbf{z}_A$ to $\mathbf{z}_* = \mathbf{0}$) by an amount $\left|\left|\mathbf{z}_A\right|\right| = \sqrt{2(r_D + r_{max})}$ in phenotype space.

Mutations occur as a Poisson process with rate U per unit time per capita, constant over time and across genotypes but potentially variable across environments. Each mutation creates a random perturbation $\mathbf{dz}$ on phenotype, which is unbiased and follows an isotropic multivariate Gaussian distribution, $\mathbf{dz} \sim N(\mathbf{0}, \lambda\, \mathbf{I}_{\boldsymbol{n}})$, where $\mathbf{I}_n$ is the identity matrix in n dimensions and λ is

the mutational variance per trait. Mutation effects add-up on *phenotype* (no epistasis), but not on *fitness* because $r(\mathbf{z})$ is nonlinear.

Figure 1 illustrates the rescue process in the FGM. At the onset of stress ($t = 0$), the optimum shifts abruptly to a new position, such that the mean growth rate becomes negative with $-r_D < 0$ (**fig 1.C**). Meanwhile, the population size starts to drop from an initial value N_0 (**fig 1.C**), facing extinction in the absence of evolution. In this context, one or several mutants or pre-existing variants may be close enough to the new optimum to have a positive growth rate ('resistant genotypes', **fig.1A,B**). These may then establish and ultimately "rescue" the population ('rescue genotypes' **fig 1.A,B**).

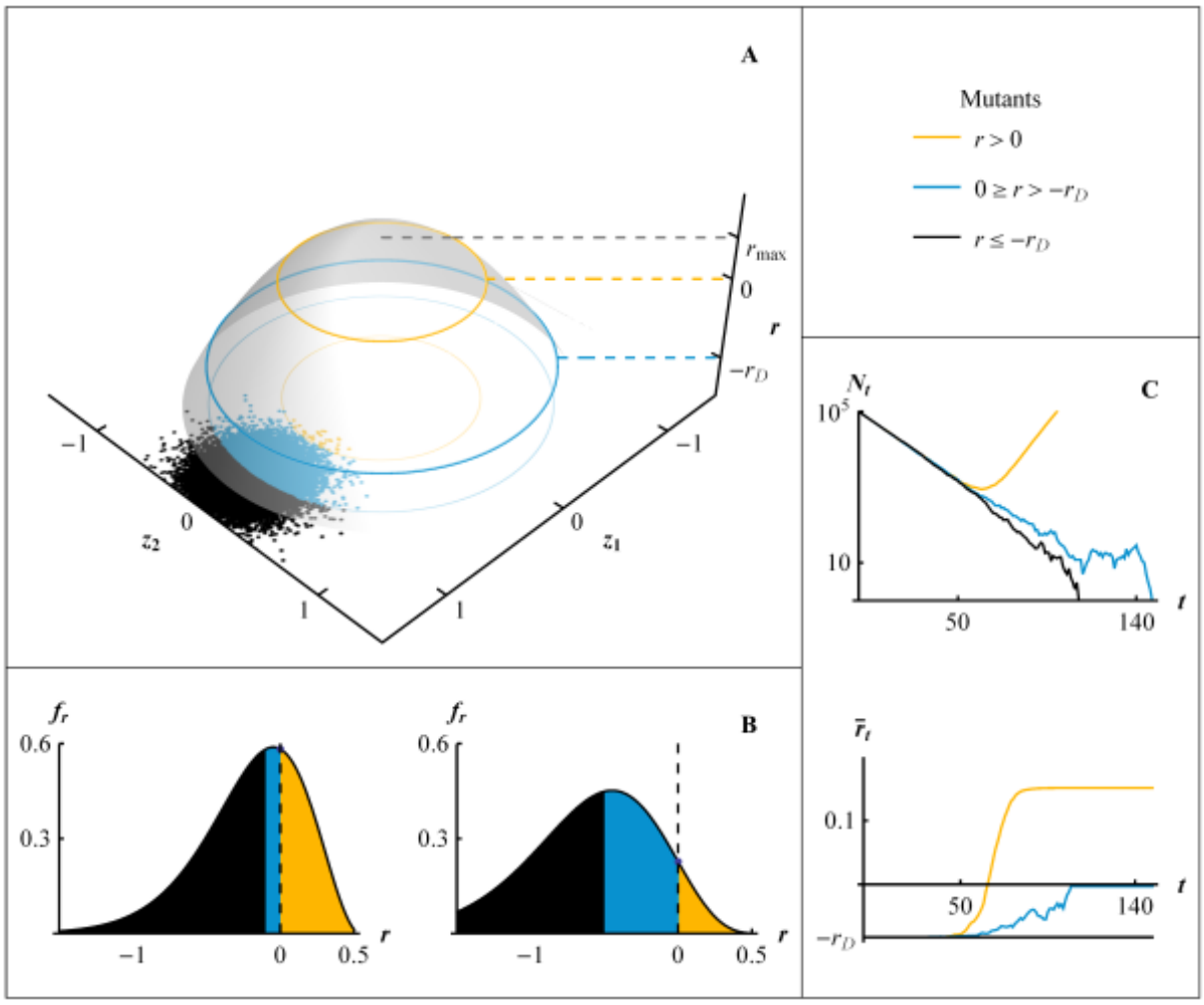

Figure 1: Evolutionary rescue in Fisher's geometric model (SSWM regime). In all panels, black refers to deleterious mutations and neutral mutations ($-r_D \geq r$), blue to beneficial but not resistant mutations ($-r_D < r < 0$) and orange to resistant mutations ($r \geq 0$). **(A)** Fitness landscape (FGM) with growth rate r (z-axis) determined by two phenotypic traits z_1 and z_2 . The growth rate of the wild-type clone in the stressful environment is $-r_D$, and r_{max} is the maximal fitness at the phenotypic optimum. **(B)** Distribution of mutation effects on growth rate (distribution of fitness effects) for the wild type with two decay rates $r_D = 0.1$ (left) and $r_D = 0.5$ (right). The colored areas give the proportions of each corresponding type of mutation. **(C)** Dynamics of the population size N_t

and mean fitness $\bar{r}_t$ of a population starting from a clone at $-r_D = -0.083$ at size $N_0 = 10^5$. The black line represents the case without fixation of a beneficial mutation, the blue line the case with extinction in spite of the fixation of a beneficial non-resistant mutation, and the orange line the case of a rescue. Parameters for the simulations are $r_{max} = 1.5$, $U = 2 * 10^{-5}$, $n = 4$ and $\lambda = 5 * 10^{-3}$.

Within the context of the FGM, increasing stress level may have different effects. First, increasing stress may involve a larger shift in the position of the optimum phenotype, resulting in a larger drop in fitness (to $-r_D$) of the formerly optimal phenotype, as assumed in most models of adaptation to a changing environment (Kopp and Matuszewski 2014). However, increasing stress may further involve a reduction in the quality of the environment, such that the maximum fitness r_{max} for the best possible phenotype is lower than in the non-stressful environment, and the absolute fitness is reduced for of all genotypes under stress. Finally, increasing stress may imply a change in the mutational parameters (U and λ), inducing shifts in evolvability. For instance, higher stress may release cryptic genetic variance on underlying phenotypic traits (Scharloo 1991; Hermisson and Wagner 2004), or cause increased mutation rates via SOS responses in bacteria (Foster 2007).

Scaled and compound parameters: It proves simpler and sufficient (see **Appendix**) to study the scaled (and unitless) growth rate $y = r/r_{max} \in [-\infty, 1]$, so that $y_D = r_D/r_{max}$ is the decay rate of the ancestor scaled to the maximum possible growth rate in the new environment. It will also prove useful to introduce another scaling by the mutational step size λ, thus introducing $\rho_D = r_D/\lambda$ and $\rho_{max} = r_{max}/\lambda$ (note that $y_D = \rho_D/\rho_{max}$). The dimensionality n of the phenotypic fitness landscape naturally arises in the formulae as $\theta = n/2$ (Martin and Lenormand 2006a). As we will see, all our results can in fact be expressed in terms of four parameters ($N_0 U$, ρ_D , ρ_{max} , θ) instead of the six original ones (U , N_0 , r_D , r_{max} , n , λ). **Table 1** summarizes all notations in the article.

Notation	Description	Formula
t	Time elapsed since onset of stress	
N_t, N_0	Population size at time t after the onset of the stress, N_0: initial population size at the onset.	
U	Mutation rate *per* individual *per* unit time.	
n, θ	n: number of traits under stabilizing selection (θ: dimensionality)	$\theta = n/2$
λ	Mutational variance induced *per* mutation on each of the n phenotypic traits	$\mathbf{dz} \sim N(\mathbf{0}, \lambda\, \mathbf{I}_n)$

U_c	Maximal mutation rate under which the WMSS regime is valid.	$U_C = \theta^2 \lambda$
$\mathbf{z}$	n-dimensional vector $\mathbf{z} \in \mathbb{R}^n$ of (breeding values for) phenotype	
$\mathbf{z}_A, \mathbf{z}_*$	$\mathbf{z}_*$: optimal phenotype in a given environment $\mathbf{z}_A$: average phenotype of the ancestral population (before the onset of stress)	$\mathbf{z}_* = \mathbf{0}$: new environment $\mathbf{z}_* = \mathbf{z}_A$: previous environment
r, σ	Growth rate (r) and reproductive variance (σ) of a given genotype, in the new environment.	$r(\mathbf{z}) = r_{max} - \lVert \mathbf{z} - \mathbf{z}_* \rVert^2/2, \mathbf{z} \in \mathbb{R}^n$(Eq.[1]) $\sigma \approx 1$
r_{max}	Maximum possible growth rate in the new environment.	$r(\mathbf{z}_*) = r_{max}$
r_D	Rate of decay of the ancestral phenotype $\mathbf{z}_A$ in the new environment.	$r(\mathbf{z}_A) = r_{max} - \lVert \mathbf{z}_A \rVert^2/2 = -r_D$
c	Scaled cost of a mutation: selective disadvantage of the mutant, relative to the optimal phenotype, in the previous environment, divided by λ.	Eq.[2]
$\tilde{c}_H$	Harmonic mean of the scaled cost among *de novo* resistant mutations.	Eq.[3],Eq. [10]
ρ_D	Rate of decay scaled by λ.	$\rho_D = r_D/\lambda$
ρ_{max}	Maximal growth rate scaled by λ.	$\rho_{max} = r_{max}/\lambda$
y	Growth rate of a genotype, in the new environment, scaled by r_{max}.	$y = r/r_{max} \in [-\infty, 1]$
$f_y(y)$	PDF of y among random single step mutations	Eq.[1]
y_D	Rate of decay scaled by r_{max}.	$y_D = r_D/r_{max} = \rho_D/\rho_{max}$
ψ_D	Alternative measure of y_D	$\psi_D = 2\left(\sqrt{1 + y_D} - 1\right)$ (Eq.[5])
α	Composite measure of stress level.	Eq.[5]
$g(\alpha)$	Function driving the dependence of rescue probabilities on stress levels.	Eq.[6]
ω_R^{DN}	Rate of rescue from *de novo* mutations scaled by $N_0\, U$	Eqs. [4],[5],[6]
ω_R^{SV}	Rate of rescue from standing variants scaled by $N_0\, U$, in an equilibrium population.	Eqs.[4],[10]
P_R	Probability of rescue.	$P_R = 1 - e^{-N_0 U\, \omega_R}$
ϕ_R^{SV}	% of rescue events caused by standing variants	Eq. [11]

Table 1: Notations

Maximal mutation rate for the SSWM regime: As we have seen, our whole approach relies on the SSWM assumption. We conjecture that this assumption should hold below some threshold mutation rate U_c, i.e. whenever $U < U_C = \theta^2 \lambda$. Indeed, Martin and Roques (2016) found that below U_C, the full fitness distribution at mutation-selection balance is exactly that expected from a single wild-type genotype at the optimum, while above U_C there is no dominant genotype in the equilibrium population. Whether this same condition is sufficient for most

rescue events to stem from single step mutations is not justified theoretically, and was simply tested by extensive stochastic simulations. **Supplementary figure 1** further explores the range of validity of this approximation. It shows, in a rescued population, the proportion of wild-type, simple mutant, double mutant, and so on, as a function of the mutation rate.

Distribution of fitness effects in the new environment: Let s be the selection coefficient (difference in growth rate), in the new environment, of a random mutant (with phenotype $\mathbf{z}$) relative to its ancestor (with phenotype $\mathbf{z}_A$). The distribution of $s = r(\mathbf{z}) - r(\mathbf{z}_A) = r + r_D$ among random mutants has a known exact form in the isotropic FGM (Martin 2014; Martin and Lenormand 2015). From it, the distribution of growth rates ($r = s - r_D$), in the new environment, is readily obtained. The scaled growth rates $y = r/r_{max}$ have the following probability density function:

$$f_y(y) = e^{-\rho_{max}(2+y_D-y)}\rho_{max}^{\theta}(1-y)^{\theta-1}\frac{{}_0F_1\left(\theta, \rho_{max}^2(1+y_D)(1-y)\right)}{\Gamma(\theta)}, \quad y \in]-\infty, 1] \qquad [2]$$

where ${}_0F_1(.,.)$ is the confluent hypergeometric function, $\Gamma(z)$ the gamma function. In the SSWM regime, this probability density function approximately describes *de novo* mutations produced after the onset of stress by the whole population, be it initially clonal or at mutation-selection balance.

Fitness distribution in the previous environment: Consider the subset of random mutations, among those that arise from the ancestral clone, that have a scaled growth rate within the infinitesimal class of scaled growth rates $[y, y + dy]$, in the new environment. Let us introduce the conditional random variable $c|y$, which is the cost (minus the selection coefficient relative to the ancestral clone), in the previous environment, of a random mutant within this subset (thus, conditional on y), and scaled by λ. Note that, because the mutation-selection balance is fully characterized by relative fitnesses, the maximal growth rate in the previous environment may differ from r_{max}, without loss of generality. Importing results from (Martin *et al.* 2013) for the SSWM regime, the total number of pre-existing variants within the class $[y, y + dy]$ is Poisson distributed with mean $N_0\ U\ \lambda\ f_y(y)/c_H(y)dy$, where $c_H(y) = 1/\mathbb{E}_c(c^{-1}|y)$ is the harmonic mean of $c|y$. This conditional harmonic mean depends on the joint distribution of fitness effects of (c, y) across two environments in the FGM (given in Martin and Lenormand 2015). In our context, the ancestral clone is optimal in the previous environment and the preexistent mutants

are closed to this ancestral clone. In this case, using results in Martin and Lenormand (2015), the resulting conditional harmonic mean $c_H(y)$ takes a tractable form (see Eq.(A6) in **Appendix**):

$$c_H(y) = 1/\mathbb{E}_c\left(\frac{1}{c}\middle|y\right) = \frac{1}{e^{v(y)}E_{\theta-1/2}\big(v(y)\big)}$$
$$\text{with } v(y) = \rho_{max}\left(2 + y_D - 2\sqrt{(1+y_D)(1-y)} - y\right), \qquad [3]$$

where $E_k(z) = \int_1^\infty e^{-z\,t}/t^k\,dt$ is the exponential integral function.

Stochastic simulations of a discrete-time model: We checked the robustness of our assumptions and approximations using stochastic simulations, where we tracked the population size and genetic composition of a population across discrete, non-overlapping generations. The size N_{t+1} of population at generation $t+1$ was drawn as a Poisson number $N_{t+1} \sim Poisson(N_t\,\overline{W})$, with $\overline{W} = \overline{e^r}$ the mean multiplicative fitness ($W = e^r$) and N_t the population size, in the previous generation. The genotypes forming this new generation were then sampled with replacement in the previous one with weight $W_i = e^{r_i}$. This is faster and exactly equivalent to drawing independent Poisson reproductive outputs for each individual, or genotype. Because of the underlying assumptions of the simulations, the corresponding analytical approximation for the stochastic reproductive variance in Eq.[1] is $\sigma \approx 1$. Mutations occurred according to a Poisson process, with a constant rate U per capita per generation. Mutation phenotypic effects were drawn from a multivariate normal distribution $N(\mathbf{0}, \lambda\,\mathbf{I_n})$, with multiple mutants having additive effects on phenotype, and their fitness computed according to the FGM (Eq.[1]).

Rescue probability was estimated by running 1000 replicate simulations until either extinction or 'rescue' occurred. A population was considered 'rescued' when it reached a population size N_t and mean growth rate $\bar{r}_t$ such that its extinction probability, if it were monomorphic, would lie bellow 10^{-6} ($\exp(-N_t\bar{r}_t) < 10^{-6}$). For rescue from populations at mutation-selection balance, 8 replicate initial equilibrium populations were generated, each by starting from an optimal clone and running the same algorithm with fixed population size ($N_t = 10^6$) until the mean Malthusian fitness stabilized to its theoretical equilibrium value $\bar{r}_{eq} = r_{max} - U$ (for $U < U_c$). Then replicate rescue simulations were performed from these initial populations as previously.

All simulations and mathematical derivations were performed in *MATHEMATICA v. 9.0* (Wolfram Research 2012).

Results

General form of the rescue probability: Extinction occurs when no resistant mutation manages to establish (i.e. to avoid stochastic loss). For compactness, we define a "rate of rescue" ω_R per individual mutant (independent of N_0 and U), such that, following (Martin *et al.* 2013), ER probabilities takes the general form: $P_R = 1 - e^{-N_0 U\, \omega_R}$. The rate of rescue from *de novo* mutations alone is ω_R^{DN} ('DN' for *de novo*), while that from pre-existing variance alone is ω_R^{SV} (for 'standing variants'). For a purely clonal population, $\omega_R = \omega_R^{DN}$, while $\omega_R = \omega_R^{DN} + \omega_R^{SV}$ when the population is initially at mutation-selection balance. Applied in the context of the FGM, the rates ω_R^{DN} and ω_R^{SV} depend on the distributions of fitness effects described in methods as follows (see **Appendix**):

$$\begin{aligned} &\omega_R^{DN} = 2/y_D \int_0^1 y\, f_y(y) dy \\ &\omega_R^{SV} = \omega_R^{DN}\ \rho_D/\tilde{c}_H \\ &\text{with } \tilde{c}_H = \int_0^1 y\, c_H(y) f_y(y) dy \Big/ \int_0^1 y\, f_y(y) dy \end{aligned} \quad . \qquad [4]$$

Because both $f_y(y)$ (Eq.[2]) and $c_H(y)$ (Eq.[3]) depend only on ρ_{max}, ρ_D and θ (and $y_D = \rho_D/\rho_{max}$), so do the two rates of rescue in Eq.[4]. This means that the growth rates of the optimal genotype (r_{max}) and of the ancestor ($-r_D$) only affect ER probabilities in a way that is scaled by the variance in phenotypic effects (λ). This result is reminiscent of results regarding the proportion of beneficial mutations in the FGM which greatly depend on the mutational variance (Fisher 1930; Orr 2000).

The log-linearity of rescue probability with N_0 ($P_R = 1 - e^{-N_0 U\, \omega_R}$) has received empirical support (Martin et al. 2013). It holds whenever each individual lineage present at the onset of stress contributes independently to the rescue process (whether by being itself a rescuer, or by generating *de novo* mutants), that is, when density or frequency-dependence in selection is negligible. Log-linearity with the mutation rate U however arises here because of the SSWM regime, where multiple mutations are ignored: it might not hold at higher mutation rates (when $U > U_c$). As such, Eq.[4] makes no further assumption than the SSWM regime ($U < U_c$); it can easily be evaluated numerically to provide a general testable theory for rescue

probabilities across stress levels, in the FGM. Yet, in order to gain more quantitative/intuitive insight into the effects of stress, we now study approximate closed form for the rates in Eq.[4], focusing on *de novo* rescue first.

Weak mutation effects approximation: We now assume that mutation effects are weak relative to the maximal growth rate under stress. More precisely, we introduce $\epsilon = \rho_{max}^{-2}$ and assume that $\epsilon \ll 1$, while retaining the SSWM regime ($U < U_c = \theta^2\lambda$). Overall mutation effects are thus assumed to fall within the range: $U/\theta^2 < \lambda \ll r_{max}^2$. We further require for analytical simplifications that $y_D \geq 2\epsilon$ in the new environment, but this only excludes situations where rescue is *de facto* certain. The weak effect assumption $\lambda \ll r_{max}^2$ can alternatively be interpreted as follows (see **Appendix**): we require that the new optimum lies several mutational steps away from the subset of 'critical' phenotypes (i.e. those with growth rate $r = 0$). It means that resistant variants typically do not overshoot the optimum. This assumption is only problematic when analyzing rescue in very low quality environments where r_{max} is very low (See **Supplementary figure 6B**).

This weak effect assumption (see **Appendix**) allows substantial simplification of the probability density function $f_y(y)$ in Eq.[2] and the harmonic mean of the scaled cost $\tilde{c}_H$ in Eq.[4]. Let us first define the following variables, which depend on (ρ_D, ρ_{max}):

$$\begin{aligned} \psi_D &= 2\left(\sqrt{1+y_D} - 1\right) \\ \alpha &= \psi_D^2 \rho_{\max}/4 + 1/2 \end{aligned} \quad . \qquad [5]$$

Under the weak effect assumption ($U/\theta^2 < \lambda \ll r_{max}^2$) the rate of *de novo* rescue (Eq.[4]) is approximately

$$\begin{aligned} \omega_R^{DN} &\approx \left(\frac{1-\psi_D/(4\alpha)}{1+\psi_D/2}\right)^{\theta - 1/2} g(\alpha) \\ \text{with } g(\alpha) &= \frac{e^{-\alpha - 1/2}}{\sqrt{2}\,\alpha\,\sqrt{1+\alpha}} \end{aligned} \quad . \qquad [6]$$

Here too, the rates r_{max} and r_D only affect ER probabilities when scaled by mutation effects λ. Differentiating ω_R^{DN} in Eq.[6] with respect to the model parameters allows evaluating the sensitivity of ER probability to these parameters (**Supplementary file S1**). ER probability always increases with increasing per-trait mutational variance λ, decreasing decay rate r_D, increasing height of the fitness peak r_{max} and decreasing dimensionality ($\theta = n/2$). The effects of λ and r_{max} are expected as it is easier to 'send' mutants in the phenotype subspace corresponding to resistance ($r > 0$) when mutation effects are large (larger λ), and when this

subspace is wider (higher peak r_{max}). The effect of n is reminiscent of the "cost of complexity", which already arises in the FGM in the absence of demographic decay (Orr 2000). ER decreases with r_D due to the fast demographic decay, as in previous models, but also due to its negative impact on the proportion of resistant mutants. This latter effect of r_D might at first sight seem inconsistent with classic results on the FGM, where the proportion of beneficial mutations typically increases with maladaptation. Resistance mutations however form a typically small subset of mutations, sufficiently beneficial to grow while their ancestor decays ($s > r_D > 0$). This subset gets smaller as the decay rate increases.

Figure 2 shows the agreement between simulations (stochastic discrete time demographic model) and the analytical expressions in Eq. [6], over the full range of stress (quantified as r_D) for two r_{max} and two U over which the rescue probability varies (**Supplementary figure 3** further explores the range of validity of this approximation). Interestingly, ER probability drops sharply with stress levels (i.e. with decay rate r_D here), much more so than predicted by a context-independent model, in which $\omega_R \propto 1/r_D$ (gray lines on **Figure 2**). This stems from the fact that in the FGM, increased stress means faster decay (as in context-independent models), but also less and weaker resistance mutations. This second effect is a driving factor in the pattern of ER probabilities across stress levels in the FGM, and is dominated by the term $g(\alpha)$ in Eq. [6] as we detail below.

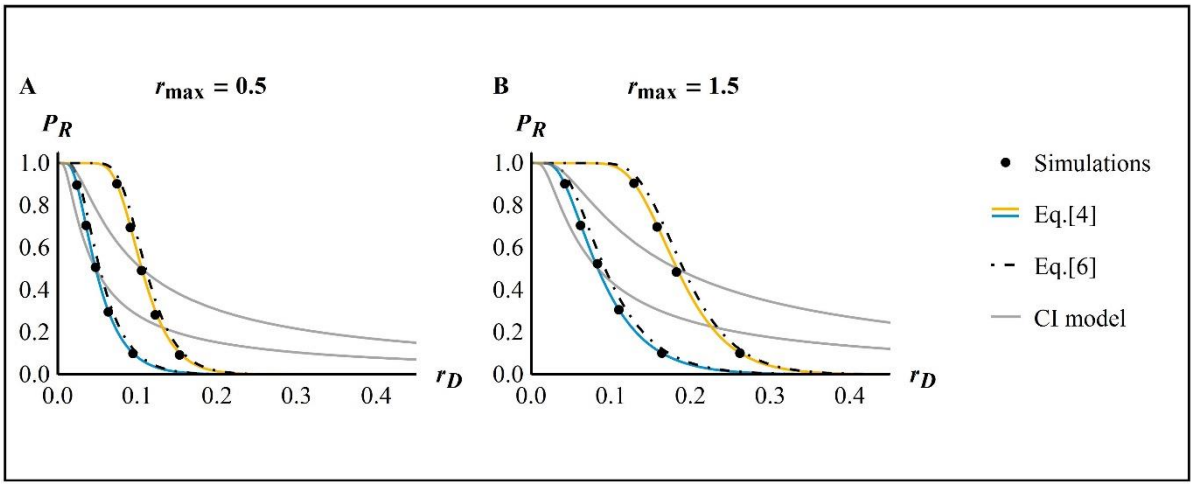

Figure 2: Rescue probability from *de novo* mutations. The ER probability as a function of stress levels, expressed as the initial mean decay rate of the population, is given for various values of the mutations rate $U = 10^{-3}\,U_c$ (blue) or $U = 10^{-2}\,U_c$ (orange) and the maximal fitness reachable in new the environment $r_{max} = 0.5$ **(A)** or 1.5 **(B)**. Dots give the results from simulations, lines (blue and orange) show the corresponding theory computed numerically (Eq.[4]). The dashed lines give the corresponding analytical approximations (Eq.[6]). The gray lines correspond to an equivalent theory without context-dependence (modified from Orr and Unckless 2008). This model was computed using a fixed proportion of resistant mutation equal to the one in Eq.[4] for a rescue

probability of 0.5 (which explain why the two curves cross exactly at $P_R = 0.5$). Other parameters are $n = 4$, $N_0 = 10^5$, $\lambda = 0.005$.

Low dimensionality/mild stress: The interplay of all parameters $(\lambda, \theta, r_D, r_{max})$ determines the stress-dependent drop in ER probability, but in a way not directly obvious from Eq.[6]. For example, the key variable ψ_D (itself roughly proportional to $y_D = r_D/r_{max}$) enters the rate of rescue in a highly nonlinear fashion.

However, the pattern simplifies substantially if dimensionality is small and/or stress is mild (y_D small). Indeed, whenever the factor $(1 - \psi_D/(4\alpha))/(1 + \psi_D/2)$ in Eq.[6] approaches 1 (the condition being less stringent as $\theta \to ½$), Eq. [6] becomes $\omega_R^{DN} \approx g(\alpha)$. Stress may in general impact all landscape parameters $(\lambda, \theta, r_D, r_{max})$, but its resulting impact on ER probabilities is then fully captured (via the function $g(.)$) by a single composite variable: α in Eq.[5]. More precisely, this simplification holds approximately, when the two following conditions are jointly verified:

$$\left.\begin{array}{l} \text{(a)}\ \ \theta - \dfrac{1}{2} \ll \dfrac{r_{max}^2}{\lambda^2} = \epsilon^{-2} \\ \text{(b)}\ \ \dfrac{2\lambda}{r_{max}} < r_D \ll 2\dfrac{r_{max}}{\theta - 1/2} \end{array}\right\} \Rightarrow\ \omega_R^{DN} \approx\ g(\alpha)\,. \qquad [7]$$

The conditions are always met in $n = 1$ dimension ($\theta - 1/2 = 0$), when $\epsilon \gg 1$ as we have assumed all along. The conditions extend to higher dimensions, as long as n remains limited (condition $(a), \theta \ll \epsilon^{-2}$) and the decay rate is small relative to the maximal growth rate (condition $(b), r_D \ll r_{max}$). Whenever conditions (a) and (b) hold, the effect of stress is entirely mediated by α and is approximately independent of dimensionality (of θ).

This simplification is illustrated in **Figure 3**, where we explore different possible effects of stress (as captured by Eq.[6]): on the maladaptation of the wild type through r_D, on the maladaptation of the wild type and the quality of the environment through r_D and r_{max} jointly, or on the maladaptation of the wild type and its evolvability through r_D and λ jointly (**Figure 3A**, blue, orange and red, resp.). These various effects are accurately summarized by a single effect of stress on α (**Figure 3B**), which is approximately independent of dimensionality (compare circles $n = 1$ and squares $n = 6$ on **Figure 3B**) and is captured by Eq.[7]. Using numerical computations from Eq.[4], instead of Eq.[6], over this wide range of parameters, leads to similar results. The range of validity of the approximation from Eq.[7] is tested more

extensively in **Supplementary figure 5**. We also note that Eq.[7] always overestimates the 'exact' ER probability from Eq.[4], so it provides a conservative bound.

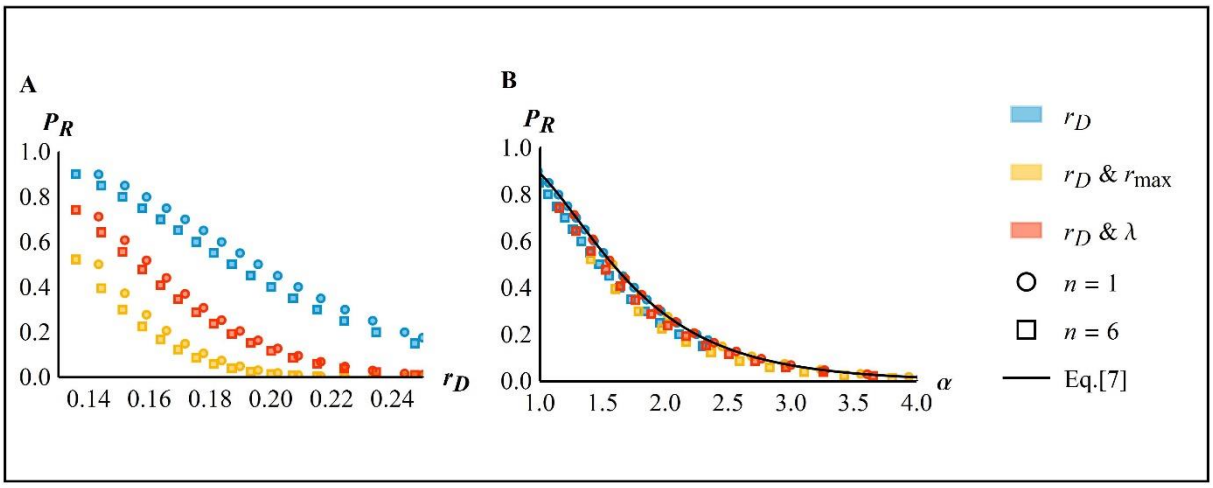

Figure 3: Composite stress measure. Rescue probability for clonal populations *vs.* initial decay rate r_D **(A)** or the composite measure of stress α **(B)**. In both panels symbols show Eq. [4] and colors refer to different effects of increased stress level: blue symbols show only r_D increasing, orange symbols r_D increasing and r_{max} decreasing linearly with r_D (according to $r_{max} = 1.5 - 5\, r_D$) and red symbols r_D increasing and λ decreasing linearly with r_D (according to $\lambda = 0.005 - 10^{-2}\, r_D$). In each case, the results for both $n = 1$ (circles) and $n = 6$ (squares) are shown. The black plain line on the left panel gives the result from Eq.[7]: a single composite measure of stress (α) approximately captures the impact of stress-induced variations in the various parameters (r_D, r_{max}, λ, n). Other parameters are $N_0 = 10^6$ and $U = 2 * 10^{-5}$.

'Characteristic stress window': From Eqs. [6]-[7], the function $g(.)$ provides a quantification of the 'window' of stress levels over which ER drops from highly likely to highly unlikely. As this drop is important in characterizing the typical range of environments in which a given population may persist, it is important to obtain analytical insight on its bounds. This is detailed in section IV of the **Appendix**, and we summarize the main results below.

We define an 'isorescue' line of a given level $p \in [0,1]$ as the set of values of parameters ($N_0, U, r_{max}, r_D, \lambda, n$) for which the rescue probability is p. At low dimensionality, from Eq.[7] we can show this isocline (for given $N_0 U$) may be characterized approximately by the set (r_{max}, r_D, λ) that corresponds to a given value of α, i.e. to $\alpha = \alpha_p = g^{-1}(N_0 U/\log(1/(1-p)))$. Using the simplification $g(\alpha) \approx \alpha^{-3/2} e^{-\alpha}/\sqrt{2e}$ (from Eq.[6] whenever $\alpha \gg 1$) this isocline can be derived explicitly (Eq. A25). Of particular relevance is the isocline of level $p = 1/2$, which defines the 'characteristic stress' $\alpha_{0.5}$ where the ER probability is $1/2$. From Eq.(A25) in section V of **Appendix**, we obtain

$$\alpha_{0.5} \underset{N_0 U \gg 1}{\approx} 0.9 \log(N_0 U) - 2.33 \,, \qquad [8]$$

where Eq.[8] applies for large $N_0 U \gg 1$ (see Appendix for a more general expression). The characteristic the stress levels $\alpha_{0.5}$ that a population can typically withstand increases only log-linearly with population size and mutation rate. Predicting how sharply the ER probability drops around the characteristic stress is also important. This drop can be characterized by a 'characteristic stress window', which we define as the range of α over which the ER probability drops from 75% to 25%. The width of this window can be scaled by the value of the characteristic stress $\alpha_{0.5}$, to get a scale-free measurement of its steepness. This simply gives

$$\frac{\Delta\alpha}{\alpha_{0.5}} \approx \frac{1}{1 + 0.7\alpha_{0.5}} \,, \qquad [9]$$

The width of the scaled "characteristic stress window" is always less than 1, and becomes small for large $\alpha_{0.5}$ (hence for large $N_0 U$ (see Eq.[8])), indicating a sharp drop in ER probability, relative to the stress level around which it occurs (as illustrated in **Figure 4**). This simple behavior described in Eq.[9] is indeed consistent with the less approximated ratio from Eq.[4] in the low dimensionality/mild stress conditions detailed in Eq.[7] (**Figure 4**).

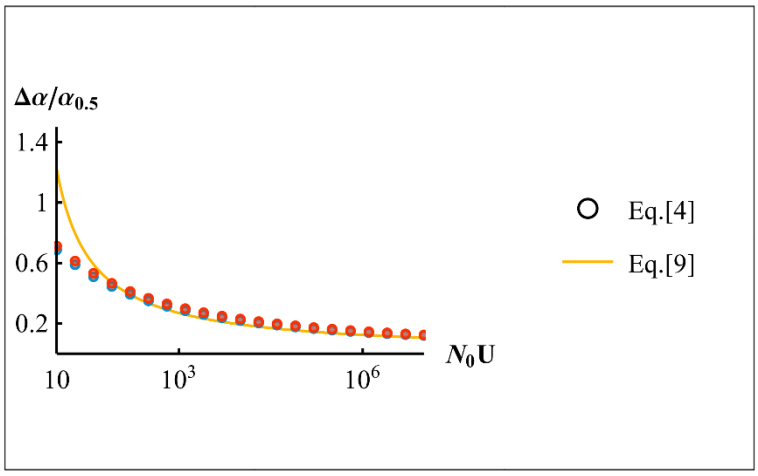

Figure 4: Scaled width of the characteristic stress window $\Delta\alpha/\alpha_{0.5}$ *vs.* the population-scale mutation rate $N_0 U$. The dots are obtained by numerical inversion of the 'exact' Eq. [4] with two values of $r_{max} = 2$ (blue) and $r_{max} = 0.1$ (red). The orange line shows the approximate characteristic scale derived in Eq.[9]. Other parameters $n = 4$, $\lambda = 0.005$.

Interestingly, Eq.[9] provides a scale-free measure that may be compared across experiments, as it only depends on the genomic mutational input $N_0 U$ (via $\alpha_{0.5}$), as seen in **Figure 4**.

However, like all results so far, eq. [9] only considers ER from *de novo* mutation. We now turn to ER from standing genetic variation.

Rate of rescue from a population at mutation-selection balance: In the SSWM regime, and for a population at mutation-selection balance in the previous environment, each rescue event can be tracked back to either a pre-existing variant, or a *de novo* mutation (Orr and Unckless 2008; Martin *et al.* 2013; Orr and Unckless 2014). The proportion ϕ_R^{SV} of rescue events caused by standing variance thus provides a natural characterization of its relative contribution to ER, and is simply given by (see **Appendix**)

$$\phi_R^{SV} = \frac{\omega_R^{SV}}{\omega_R^{DN} + \omega_R^{SV}} = \frac{\rho_D}{\tilde{c}_H + \rho_D} \underset{\substack{r_{max} \gg \lambda \\ \alpha \geq 1}}{\approx} \frac{\rho_D}{\theta + \alpha + \rho_D}. \qquad [10]$$

The right-hand side expression corresponds to the weak effect approximation ($\rho_{max} \gg 1$) with substantial stress ($\alpha \geq 1$), in which case $\tilde{c}_H \approx \theta + \alpha$. The ER probability is $P_R = 1 - e^{-N_0 U \omega_R}$ where $\omega_R = \omega_R^{DN} + \omega_R^{SV} = \omega_R^{DN}/(1 - \phi_R^{SV})$. **Figure 5A** shows how P_R varies with stress (here, increasing r_D), in the presence of standing variance, and the agreement between simulations and closed form expressions from Eq.[4] and [11]. It is apparent from eq. [10] and in **Figure 5B** that the contribution from standing variance in large r_D (low ER probability from *de* novo mutations) is dominant when available ($\lim_{r_D \to \infty} \phi_R^{SV} = 0.5$ from Eq.[10]) but decreases ($\lim_{r_D \to 0} \phi_R^{SV} = 0$ from Eq.[10]) for very low stress (ER probability from *de* novo mutations is highly likely).

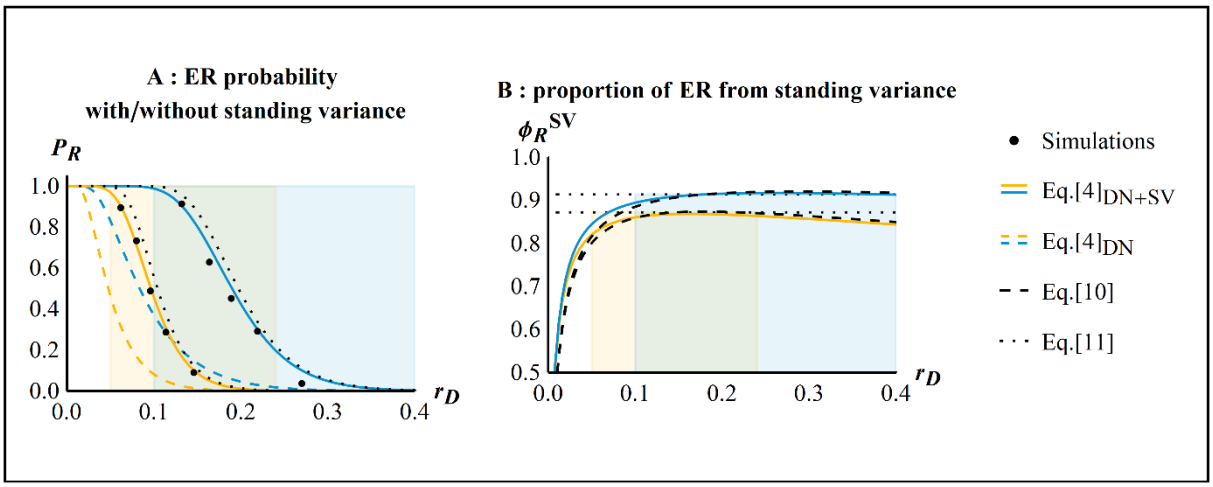

Figure 5: **ER probability in the presence of standing genetic variation.** In each panel, orange and blue correspond to two values of the maximal fitness in the new environment: $r_{max} = 0.5$ or 1.5 (respectively). Stress only affects the decay rate r_D(shifting optimum). **(A)** ER probability in the presence of standing genetic variation

as a function of stress level r_D: simulations (dots) vs. corresponding theory (dashed and plain lines, see legend) for either *de novo* rescue alone ('DN') or *de novo* plus standing variance ('DN'+'SV'). The dotted black line gives the simpler expression for the overall rescue rate: $\omega_R \approx \omega_R^{DN}/(1-\phi_R^*)$, from ϕ_R^* in Eq.[11]. **(B)** Proportion of rescue from standing variance as a function of r_D: the lines give the corresponding theory, based on $\tilde{c}_H$ in Eq. [4] or on $\tilde{c}_H \approx \theta + \alpha$ (approximation in Eq. [10]). Each colored shaded area (orange or blue, and green when overlapping) shows, for the corresponding value of r_{max} (0.5 or 1.5 respectively), the range of r_D for which ER probability drops from 0.99 to 10^{-3}. Other parameters: $n = 4, N_0 = 10^5, \lambda = 0.005$.

We observe a very similar drop in ER probability with stress as with *de novo* mutation (**Figure 5A**), but at higher 'characteristic stress'. **Figure 5B** shows that ϕ_R^{SV} is maximal at intermediate stress levels, as captured both by the approximation $\phi_R^{SV} \approx \rho_D/(\theta + \alpha + \rho_D)$ (dashed lines) and the more exact expression based on ω_R^{DN} and ω_R^{SV} in Eq.[4] (plain lines). This stems from the nonlinearity of the cost of resistance ($\tilde{c}_H$) with ρ_D in Eq. [10]. At very mild stress, rescue stems from mild effect mutations, the cost of which is roughly independent of ρ_D (Martin and Lenormand 2015). Thus, their contribution is roughly stable across mild stress levels, while that from *de novo* mutations decreases with stress (as $1/\rho_D$). Overall, rescue stems more from standing variants as ρ_D increases, in this range. At very large stress levels, rescue stems from strong effect mutations: these pay a substantial 'incompressible cost' (Martin and Lenormand 2015), that increases faster than ρ_D. Therefore, the contribution from standing variants decreases again with stress, in this range (remaining dominant: $\phi_R^{SV} \geq 1/2$).

However, the variation of ϕ_R^{SV} may be negligible in practice. Assume a large $N_0\ U$ and that stress only affects ρ_D (rather than ρ_{max} or θ). Then over a wide range of stress levels (shaded area), ϕ_R^{SV} is close to maximal and roughly constant (**Figure 5B**). In our illustration, this range covers $P_R \sim 0.99$ to $P_R \sim 10^{-3}$. Mathematically, the curvature of ϕ_R^{SV} with r_D is limited around its maximum value (of order $\rho_{max}^{-2} = \epsilon^2$, see **Appendix**), when P_R only varies with ρ_D. Overall, over a large range of stress level in which ER probability falls from highly likely to highly unlikely, ϕ_R^{SV} hardly deviates from its maximal value ϕ_R^*, which is given below (dotted line in **Figure 5B**). This means that the rate of rescue with standing variance is approximately proportional to that with only *de novo* mutation, with constant proportionality largely independent of the stress level:

$$\phi_R^{SV} \approx \phi_R^* = \max_{\rho_D \in \mathbb{R}^+} \phi_R^{SV} \approx \frac{1}{1 + 0.7\,(\theta/\rho_{max})^{0.4}}\ . \qquad [11]$$
$$\omega_R = \omega_R^{DN} + \omega_R^{SV} \approx\ \omega_R^{DN}/(1-\phi_R^*)$$

This constant contribution from standing variance decreases with increasing dimensionality (θ) and with a lower fitness peak (ρ_{max}). The rough constancy of ϕ_R^{SV} also means that all the results

obtained previously for *de novo* ER apply in the presence of standing variance, when stress only shifts the optima. The characteristic stress is higher (replacing U by $U/(1-\phi_R^*)$ in Eq.[8]), with the same profile (stress window), as captured by the approximation $\omega_R \approx \omega_R^{DN}/(1-\phi_R^*)$ (Eq. [11], dotted black line in **Figure 5A**).

Finally, note that U may also change across environments, from U_P (for previous) to U_N (for new). In the SSWM regime, this would simply amount to replacing $\tilde{c}_H$ by $\tilde{c}_H\ U_N/U_P$ (in Eq. [10]). For example, a stress-induced increase in DNA copy error would yield $U_N > U_P$ and a larger contribution from *de novo* mutation (lower ϕ_R^{SV} in Eq.[10]). On the contrary, a decrease in birth rate in the stress, combined with birth-dependent mutation (as is typical in microbes) would imply $U_N < U_P$ and a larger contribution from standing variance (higher ϕ_R^{SV} in Eq.[10]).

Discussion

Main results: We investigated the persistence of a population of asexual organisms under an abrupt environmental alteration. This 'stress' affects a single peak fitness landscape (FGM), which the population must 'climb' to avoid extinction. A quantitative constraint arises from this landscape, linking the initial decay rate of the population, the proportion and growth rate of resistance alleles among random mutants, and their selective cost before stress. In the model, a continuum of stress levels may modify the landscape in various ways: shifting the optimum, changing the peak height or the phenotypic scale of mutations. Under a SSWM regime and assuming weak mutation effects, all these effects are approximately captured by the variation, across stress levels, of a single composite parameter α (Eq. **[6], Figure 3, Figure 4, Supplementary figure 4**). The probability of ER drops sharply with the measure of stress α (Eq.[9], **Figure 4**), more so than in previous context-independent models (**Figure 2**). The 'characteristic stress window', over which this drop occurs, only depends on N_0U: as N_0U gets larger, the window gets narrower (**Figure 4**) and shifts towards higher stress levels, approximately as $\log(N_0U)$ (Eq.[8]). When standing variance is available (population at equilibrium before stress), its contribution to ER is dominant and approximately constant across stress levels (Eqs.[10]-[11], **Figure 5**), in this same regime (SSWM and weak mutation effects).

Empirical implications for the evolution of resistance: In chemotherapy, stress level is the main factor under our control (dose regimes etc.). Empirically, it is also perhaps the best-studied

factor in this context (Gunderson *et al.* 2001; Drusano 2004). Therefore, it seems important to provide a predictive model of ER probabilities over a range of stress levels comparable to experimental data in order to give insights into the complex trade-off between curing infections and managing resistance (Day and Read 2016; Levin-Reisman *et al.* 2017). In general, to test our predictions and any ER model, it is critical to empirically relate physical measures of stress level (e.g. concentrations, temperatures, salinities etc.) with demographic measures (decay rates). Here we consider, for example, the concentration υ of an antibiotic. With such data our model could be tested in several ways. First, assuming that increased υ only implies larger shifts in the optimum, then only r_D depends on υ. This parameter ($r_D(\upsilon)$) can be measured over a range of concentrations via classic kill-curve studies (Regoes *et al.* 2004). The probability of resistance emergence ($P_R(\upsilon)$), from a purely clonal population, can also be measured across the same range of υ. We then expect a predictable relationship between $P_R(\upsilon)$ and $r_D(\upsilon)$, which could depend on other parameters as r_{max}, λ or even U according to the model considered (Eqs.[6][7][10]).

For a more powerful test of the model, the full set of parameters may be inferred from additional measures. The FGM parameters (λ, θ, assumed constant across υ) and mutation rate U may be estimated from random mutation data in the model species considered (Martin and Lenormand 2006b; Perfeito *et al.* 2014). The maximal growth rate in the stress would ideally have to be measured on lines well-adapted to each particular concentration υ (e.g. Harmand et al. *submitted*). If too challenging, this last parameter could be assumed constant and estimated from the $P_R$vs r_D relationship. An alternative use of our results is to infer the parameter $\alpha(\upsilon)$ across concentrations υ, from the observed relationship $P_R(\upsilon)$, given a known value of N_0U, by inverting $g(\alpha)$ (assuming limited dimensionality, Eq.[7]). Finally, the simple scale free characterization of the characteristic stress window (Eqs.[9]) could be tested across various inoculum sizes (i.e. across N_0U).

Density-dependence and competitive release: Our model ignores density dependence but it could be introduced easily. *A minima*, one could consider a single density dependence coefficient (common to all genotypes) and use logistic diffusion approximations (Lambert 2005). This would potentially allow for 'competitive release' effects (Read *et al.* 2011). Such effects are expected in density-dependent models when resistant variants are present before stress. Then higher stresses may actually favor the emergence of resistance by rapidly depleting the sensitive wild-type population, thus releasing limiting resources for resistant genotypes.

Previous models that showed competitive-release effects assumed context-independent mutation (Read *et al.* 2011; Day and Read 2016), where the number of standing resistant mutants is independent of stress level. Thus, increased stress mostly limits *de novo* rescue mutation with more limited impact on the contribution from standing variance. On the contrary, the FGM imposes a similar drop, with stress, in the rate of rescue from *de novo* and preexisting mutants (Eq.[11]).The positive effects of competitive release on ER probability may thus be less important, in the FGM, than predicted from these previous models.

Small peak limit: In the "weak mutation effect limit" (Eqs. [6]-[7]), resistant mutants are typically much less fit that the optimal phenotype in the stress ($r \ll r_{max}$). They belong to the *tail* of the mutant phenotypic distribution and are packed in the portion of the subspace of all resistant phenotypes closest to the ancestor (see **Supplementary figure 6A**). An alternative situation (still described by Eq.[4] but not Eqs. [6]-[7]) is when resistant mutants typically cover the whole subspace of resistance phenotypes, but this subspace is very small (so that ER remains unlikely). This situation (illustrated in **Supplementary figure 6A**) corresponds to a case where mutation effects are similar or larger than the maximal growth rate ($\lambda = O(r_{max})$). The fitness peak in the stress is then not very high (r_{max} is small), and mutations can easily overshoot the optimum in the new environment. In this situation, at least for mild decay rates, resistant phenotypes are a small subset from the *bulk* of the mutant phenotypic distribution. The volume (in phenotype space) occupied by this subset is roughly constant across stress and determines the ER probability, together with decay rate (by a direct demographic effect). The cost of complexity is more important in this regime, as it strongly determines the volume of the resistance subspace (see **Supplementary figure 6B**).

Anisotropy and parallel evolution in drug resistance: The present model is isotropic, in that all directions in phenotype space are equivalent (in terms of mutation and selection). Yet, in general, module – dependent anisotropy (where particular genes mutate along favored directions) is the key requirement for the FGM to generate substantial parallel evolution (Chevin 2013). Parallel evolution, whereby some (portions or sets of) genes contribute most of the resistance mutations, is often observed among drug resistance alleles, and can further increase with stress (Harmand *et al.* 2016). Although not explored here, we conjecture that our model may accommodate some anisotropic extensions. First, mild anisotropy (even environment-dependent) might have limited impact. If mutational covariances between traits

merely “turn”, “shrink” or “expand” the phenotypic mutant cloud, this would approximately amount to a mere change in λ in an equivalent isotropic landscape (Martin and Lenormand 2006a; Martin 2014). Second, a particular form of strong anisotropy may arise when mutant phenotypes (in a given module) spread along a single favored direction (Martin 2014). It may then be sufficient to reduce the n dimensional model to a single dimension version of the present isotropic model ($n = 1$: Eq.[7] is then exact). This conjecture would require further investigation.

Robustness of the limiting assumptions: Several limiting assumptions of the evolutionary model used here can be justified by the short timescale and rarity of rescue events. Assuming a single optimum seems reasonable in a harsh environment: most rescue trajectories will *a priori* stem from the few mutants reaching the closest local optimum in the landscape. The use of the SSWM approximation also seems reasonable in the context of rescue. Indeed, mutants that show substantial decay rates do not persist long enough in the population to contribute much secondary mutations (Martin *et al.* 2013). This argument applies if the genomic mutation rate is low enough (roughly $U < U_c = \theta^2\lambda$, **Supplementary figure 1**). In contexts where the mutation rate is higher (e.g. viruses or mutator bacterial strains), multiple mutants must be accounted for as a source of ER. These can in principle be introduced in the framework used here (Martin *et al.* 2013), but, especially when applied to the FGM, the results quickly become intractable. Alternative population genetics assumptions would have to be used, which is beyond the scope of this work.

Conclusion: Recently, the FGM has received renewed interest by its ability to provide testable, quantitative and often accurate predictions regarding patterns of mutation effects on fitness, across various species and contexts (Tenaillon 2014). The present model is an attempt to extend its scope to model the evolution of resistance to stress. We hope that future experimental tests will evaluate its accuracy and potential to tackle pressing applied issues, in particular regarding resistance management.

Bibliography

Agrawal A. F., Whitlock M. C., 2010 Environmental duress and epistasis: how does stress affect the strength of selection on new mutations? Trends Ecol. Evol. 25: 450–458.

Alexander H. K., Martin G., Martin O. Y., Bonhoeffer S., 2014 Evolutionary rescue: linking theory for conservation and medicine. Evol. Appl. 7: 1161–1179.

Bijlsma R., Loeschcke V., 2005 Environmental stress, adaptation and evolution: an overview. J. Evol. Biol. 18: 744–749.

Burger R., Lynch M., 1995 Evolution and Extinction in a Changing Environment: A Quantitative-Genetic Analysis. Evolution 49: 151.

Carlson S. M., Cunningham C. J., Westley P. A. H., 2014 Evolutionary rescue in a changing world. Trends Ecol. Evol. 29: 521–530.

Charmantier A., Garant D., 2005 Environmental quality and evolutionary potential: lessons from wild populations. Proc. R. Soc. B Biol. Sci. 272: 1415–1425.

Chevin L.-M., 2011 On measuring selection in experimental evolution. Biol. Lett. 7: 210–213.

Chevin L.-M., 2013 GENETIC CONSTRAINTS ON ADAPTATION TO A CHANGING ENVIRONMENT. Evolution 67: 708–721.

Davies J., Davies D., 2010 Origins and Evolution of Antibiotic Resistance. Microbiol. Mol. Biol. Rev. 74: 417–433.

Day T., Read A. F., 2016 Does High-Dose Antimicrobial Chemotherapy Prevent the Evolution of Resistance? PLoS Comput. Biol. 12: e1004689.

De Visser J. a. G. M., Rozen D. E., 2005 Limits to adaptation in asexual populations. J. Evol. Biol. 18: 779–788.

Drlica K., 2003 The mutant selection window and antimicrobial resistance. J. Antimicrob. Chemother. 52: 11–17.

Drusano G. L., 2004 Antimicrobial pharmacodynamics: critical interactions of “bug and drug.” Nat. Rev. Microbiol. 2: 289–300.

Feller W., 1951 Diffusion processes in genetics. In: *Proceedings of the Second Berkeley Symposium on Mathematical Statistics and Probability*,

Fisher R. A., 1930 *The Genetical Theory of Natural Selection*. Oxford University Press.

Foster P. L., 2007 Stress-Induced Mutagenesis in Bacteria. Crit. Rev. Biochem. Mol. Biol. 42: 373–397.

Gillespie J. H., 1983 Some Properties of Finite Populations Experiencing Strong Selection and Weak Mutation. Am. Nat. 121: 691–708.

Gomulkiewicz R., Holt R. D., 1995 When does Evolution by Natural Selection Prevent Extinction? Evolution 49: 201.

Gomulkiewicz R., Holt R. D., Barfield M., Nuismer S. L., 2010 Genetics, adaptation, and invasion in harsh environments. Evol. Appl. 3: 97–108.

Gonzalez A., Bell G., 2013 Evolutionary rescue and adaptation to abrupt environmental change depends upon the history of stress. Philos. Trans. R. Soc. Lond. B Biol. Sci. 368: 20120079.

Gonzalez A., Ronce O., Ferriere R., Hochberg M. E., 2013 Evolutionary rescue: an emerging focus at the intersection between ecology and evolution. Philos. Trans. R. Soc. B Biol. Sci. 368: 20120404–20120404.

Gunderson B. W., Ross G. H., Ibrahim K. H., Rotschafer J. C., 2001 What Do We Really Know About Antibiotic Pharmacodynamics? Pharmacother. J. Hum. Pharmacol. Drug Ther. 21: 302S–318S.

Harmand N., Gallet R., Jabbour-Zahab R., Martin G., Lenormand T., 2016 Fisher's geometrical model and the mutational patterns of antibiotic resistance across dose gradients. Evolution: 1–32.

Hermisson J., Wagner G. P., 2004 The Population Genetic Theory of Hidden Variation and Genetic Robustness. Genetics 168: 2271–2284.

Hietpas R. T., Bank C., Jensen J. D., Bolon D. N. A., 2013 Shifting Fitness Landscapes in Response to Altered Environments. Evolution 67: 3512–3522.

Hoffmann A. A., Parsons P. A., 1997 *Extreme environmental change and evolution*. Cambridge University Press, Cambridge; New York.

Hoffmann A. A., Merilä J., 1999 Heritable variation and evolution under favourable and unfavourable conditions. Trends Ecol. Evol. 14: 96–101.

Koehn R. K., Bayne B. L., 1989 Towards a physiological and genetical understanding of the energetics of the stress response. Biol. J. Linn. Soc. 37: 157–171.

Kopp M., Matuszewski S., 2014 Rapid evolution of quantitative traits: theoretical perspectives. Evol. Appl. 7: 169–191.

Lambert A., 2005 The branching process with logistic growth. Ann. Appl. Probab. 15: 1506–1535.

Levin-Reisman I., Ronin I., Gefen O., Braniss I., Shoresh N., *et al.*, 2017 Antibiotic tolerance facilitates the evolution of resistance. Science: eaaj2191.

Lindsey H. A., Gallie J., Taylor S., Kerr B., 2013 Evolutionary rescue from extinction is contingent on a lower rate of environmental change. Nature 494: 463–467.

Lynch M., Gabriel W., Wood A. M., 1991 Adaptive and demographic responses of plankton populations to environmental change. Limnol. Oceanogr. 36: 1301–1312.

MacLean R. C., Perron G. G., Gardner A., 2010 Diminishing Returns From Beneficial Mutations and Pervasive Epistasis Shape the Fitness Landscape for Rifampicin Resistance in Pseudomonas aeruginosa. Genetics 186: 1345–1354.

Martin G., Lenormand T., 2006a A General Multivariate Extension of Fisher's Geometrical Model and the Distribution of Mutation Fitness Effects Across Species. Evolution 60: 893–907.

Martin G., Lenormand T., 2006b The Fitness Effect of Mutations Across Environments: A Survey in Light of Fitness Landscape Models. Evolution 60: 2413–2427.

Martin G., Elena S. F., Lenormand T., 2007 Distributions of epistasis in microbes fit predictions from a fitness landscape model. Nat. Genet. 39: 555–560.

Martin G., Aguilée R., Ramsayer J., Kaltz O., Ronce O., 2013 The probability of evolutionary rescue: towards a quantitative comparison between theory and evolution experiments. Philos. Trans. R. Soc. Lond. B. Biol. Sci. 368: 20120088.

Martin G., 2014 Fisher's geometrical model emerges as a property of complex integrated phenotypic networks. Genetics 197: 237–255.

Martin G., Lenormand T., 2015 The fitness effect of mutations across environments: Fisher's geometrical model with multiple optima. Evolution 69: 1433–1447.

Martin G., Roques L., 2016 The Non-stationary Dynamics of Fitness Distributions: Asexual Model with Epistasis and Standing Variation. Genetics: genetics.116.187385.

Moser C., Bell G., 2011 Genetic correlation in relation to differences in dosage of a stressor. J. Evol. Biol. 24: 219–223.

Orr H. A., 2000 Adaptation and the Cost of Complexity. Evolution 54: 13–20.

Orr H. A., Unckless R. L., 2008 Population extinction and the genetics of adaptation. Am. Nat. 172: 160–9.

Orr H. A., Unckless R. L., 2014 The Population Genetics of Evolutionary Rescue. PLOS Genet. 10: e1004551.

Perfeito L., Sousa A., Bataillon T., Gordo I., 2014 Rates of Fitness Decline and Rebound Suggest Pervasive Epistasis. Evolution 68: 150–162.

Read A. F., Day T., Huijben S., 2011 The evolution of drug resistance and the curious orthodoxy of aggressive chemotherapy. Proc. Natl. Acad. Sci. 108: 10871–10877.

Regoes R. R., Wiuff C., Zappala R. M., Garner K. N., Baquero F., *et al.*, 2004 Pharmacodynamic Functions: a Multiparameter Approach to the Design of Antibiotic Treatment Regimens. Antimicrob. Agents Chemother. 48: 3670–3676.

Remold S. K., Lenski R. E., 2001 Contribution of individual random mutations to genotype-by-environment interactions in Escherichia coli. Proc. Natl. Acad. Sci. U. S. A. 98: 11388–11393.

Remold S. K., Lenski R. E., 2004 Pervasive joint influence of epistasis and plasticity on mutational effects in Escherichia coli. Nat. Genet. 36: 423–426.

Samani P., Bell G., 2010 Adaptation of experimental yeast populations to stressful conditions in relation to population size. J. Evol. Biol. 23: 791–796.

Scharloo W., 1991 Canalization: genetic and developmental aspects. Annu. Rev. Ecol. Syst. 22: 65–93.

Sgrò C. M., Hoffmann A. A., 2004 Genetic correlations, tradeoffs and environmental variation. Heredity 93: 241–248.

Tenaillon O., 2014 The Utility of Fisher's Geometric Model in Evolutionary Genetics. Annu. Rev. Ecol. Evol. Syst. 45: 179–201.

Trindade S., Sousa A., Gordo I., 2012 Antibiotic Resistance and Stress in the Light of Fisher's Model. Evolution 66: 3815–3824.

Turelli M., 1984 Heritable genetic variation via mutation-selection balance: Lerch's zeta meets the abdominal bristle. Theor. Popul. Biol. 25: 138–193.

Uecker H., Otto S. P., Hermisson J., 2014 Evolutionary Rescue in Structured Populations. Am. Nat. 183: E17–E35.

Uecker H., Hermisson J., 2016 The Role of Recombination in Evolutionary Rescue. Genetics 202: 721–732.

Wang A. D., Sharp N. P., Spencer C. C., Tedman-Aucoin K., Agrawal A. F., 2009 Selection, Epistasis, and Parent-of-Origin Effects on Deleterious Mutations across Environments in *Drosophila melanogaster*. Am. Nat. 174: 863–874.

Wang A. D., Sharp N. P., Agrawal A. F., 2014 Sensitivity of the Distribution of Mutational Fitness Effects to Environment, Genetic Background, and Adaptedness: A Case Study with Drosophila. Evolution 68: 840–853.

Wolfram Research I., 2012 *Mathematica*. Wolfram Research, Inc, Champaign, Illinois.